Received: 18 March 2022 | Revised: 6 July 2022 | Accepted: 6 July 2022

DOI: 10.1049/els2.12047

IET Electrical Systems in Transportation

The Institution of Engineering and Technology WILEY

ORIGINAL RESEARCH

Intermittent series direct current arc fault detection in direct current more-electric engine power systems based on wavelet energy spectra and artificial neural network

J. Thomas | R. Telford | P. J. Norman | G. M. Burt

Electronics and Electrical Engineering Department, University of Strathclyde, Glasgow, UK

Correspondence

J. Thomas, Electronics and Electrical Engineering Department, University of Strathclyde, 99 George St, G1 1RD, Glasgow, UK.
Email: jeffy.johny@strath.ac.uk

Abstract

The move towards More-Electric Aircraft (MEA) and Engine (MEE) systems has resulted in system integrators exploring the use of Direct Current (DC) for primary power distribution to both reduce energy conversion stages and enable parallelling of non-synchronised engine off-take generation. A prevalent challenge of utilising DC systems is the safe management of arc faults. Arcing imposes a significant threat to aircraft and can result in critical system damage. Series intermittent arc faults in DC systems are particularly challenging to detect due to the lack of a zero current crossing coupled with the intermittency caused by in-flight vibrations. Additionally, several state-of-the-art arc fault detection methodologies fail to address the handling of aircraft system-specific conditions such as dynamic loading and stability requirements. This paper addresses these unique MEA/MEE issues through the proposal of a new generalised real-time arc fault detection methodology (WaSp) based on time–frequency domain-extracted features applied to a feed-forward Artificial Neural Network (ANN). The paper outlines the analysis of arc fault time–frequency domain features. Simulation-based case studies emulating a range of on-board EPS conditions are presented and show the proposed system has the potential for highly accurate and generalised detection performance with fast detection times.

1 | INTRODUCTION

The more-electric aircraft (MEA) concept, where hydraulic and pneumatic aircraft sub-systems are replaced with electrical equivalents, is anticipated to reduce operational costs [1] and improve overall security, reliability and energy efficiency of future aircraft [2]. Similarly, the more-electric engine (MEE) concept, where conventional mechanically driven engine auxiliary subsystems are replaced with electrical counterparts, is also being considered.

In general, future MEA and MEE systems are expected to have higher capacity, higher voltage, electrical power systems (EPS) that feature a greater utilisation of advanced power electronic conversion technologies and DC distribution. These changes have resulted in a variety of emerging operational and design challenges that must be considered to maintain high reliability and meet the safety standards required for certification. This paper considers the challenge of accurately detecting intermittent series arc faults within DC systems of future MEE/MEA.

Aircraft electrical systems are often subjected to extreme environmental conditions. Arc faults may arise as a result of degraded wires being in contact with metal structures or the vibration of loose terminal connections, and are likely to follow an intermittent nature [3]. Within AC systems, the natural current-zero crossings result in an arc event being naturally quenched, with arc reignition being subject to electrode gap length and ionisation conditions. However, in DC systems, due to the absence of zero-crossings in current profiles [4], arc faults may be sustained for much greater durations. The heat produced during arcing events presents a significant fire risk to surrounding insulation, affecting overall system safety and

This is an open access article under the terms of the Creative Commons Attribution License, which permits use, distribution and reproduction in any medium, provided the original work is properly cited.

© 2022 The Authors. *IET Electrical Systems in Transportation* published by John Wiley & Sons Ltd on behalf of The Institution of Engineering and Technology.

reliability. One such example is the fire event that transpired as a result of a chaffed power feeder cable in a Lockheed Martin F-22 development aircraft which ultimately resulted in the loss of the aircraft [5]. Furthermore, conventional overcurrent and current differential methods do not provide reliable coverage against arc faults due to the potentially reduced fault current levels.

While detection methods are proposed within literature [6], there are still outstanding issues concerning intermittency of arcing, applicability to MEA/MEE systems, and balancing the trade-off between detection speed and accuracy. Moreover, the need for reliable series DC arc fault detection will extend to all-electric and hybrid-electric propulsion systems, where the severity of arcing conditions will likely be exacerbated by the use of higher voltage platforms.

This paper proposes a real-time generalised detection methodology combining elements of time–frequency domain-based features and a feed forward artificial neural network (ANN) [7] that can accurately identify the occurrence of intermittent series arc faults during a wide range of dynamic MEE load conditions. A further contribution is provided with detailed analysis of time–frequency extracted features under arcing and normal conditions.

The paper is organised as follows; an overview of the principles of arc faults and associated detection challenges is first presented, followed by a review of state-of-the-art arc fault detection (AFD) methods used across a wide range of power system applications. A novel detection system, named WaSp (derived from Wavelet Spectra, the methodology it is based on) is then proposed which addresses several challenges identified through the literature review, and multiple simulation-based case studies are presented to validate the performance of the proposed method. WaSp's novelty lies in combining utilisation of Discrete Wavelet Transform and Parseval's energy theorem to obtain fault discriminant features that support series intermittent AFD under varying load conditions. A discussion is then provided comparing WaSp with current state of the art AFD techniques from the literature.

2 | SERIES DC ARC FAULTS

2.1 | All arc fault formation

Electrical arcs are self-sustaining electric discharges across an air gap formed between two electrodes. Ionisation occurs in the air gap between the conductors such that their voltage difference exceeds the dielectric breakdown voltage, resulting in arc initiation [8]. Normal arcing events are a result of mechanical switching operations and generally exhibit highly transient and unsustainable behaviour. Circuit breakers (CBs) and mechanical switching devices in general are designed to withstand their development.

However, arc current as a result of ionised gas during fault events can result in fully sustained arcing, and the subsequent heat generation can pose a fire risk to the neighbouring insulation. Arc faults are characterised as either parallel or series. Parallel arc faults occur between two phases or a phase conductor and ground and are considered a form of high impedance short circuit. Series faults conditions occur in series with loads and are usually a result of loose terminal connections [9]. During series arc conditions there is an effective reduction in load current because of the additional series impedance introduced to the circuit. Consequently, current levels may drop below the rated levels and significantly below relay time-current curves, thus negating conventional overcurrent and current differential methods. Furthermore, vibration during aircraft operating conditions can result in intermittent fault behaviour at loose terminal connections. It has been demonstrated in AC systems that a single intermittent arc event may last for approximately 1.25 ms with a series of events extending to 20–30 ms [10] although there have been limited studies on intermittency within DC systems.

A range of methods and devices exist for detecting and isolating AC parallel arc fault conditions [11]. However, to date, advanced technology for the detection of series DC faults has not been as fully developed [12], and considering the trend towards future MEA/MEE systems embracing DC-based distribution systems, there is significant ongoing research into highly reliable and discriminative series DC arc fault detection. Also, dynamic load conditions in future MEA/MEE EPS will challenge a detection system's ability to accurately discriminate between true fault events and transient load changes. The following section discusses existing methods proposed in literature for diagnosis of series DC arc faults.

2.2 | Fault detection and isolation methodologies

A range of methods have previously been proposed for the detection of series arc faults [6]. Systems for detection are generally classified depending on the data features that are extracted and used for discrimination: methods based on time [13], frequency [14] and time–frequency domain extracted features have been previously proposed.

Time domain-based AFD in DC systems [15, 16] are comprised of methods that analyse current and voltage signals for behavioural changes, such as within 3-phase imbalances, feeder voltages, arc fault energy etc. The associated limitations of time domain AFD mainly concern the challenge of defining suitable thresholds and features for accurate detection and sensitivity in the presence of masking conditions such as capacitor inrush and load switching transients.

Frequency domain AFD methods [17, 18] are generally based on the analysis of voltage and current frequency spectra extracted using the Fast Fourier Transform (FFT). Momoh and Button [19] combined the FFT of current and voltage signals with an artificial neural network (ANN) for detection purposes. Gu et al. [20], proposed and implemented an algorithm that evaluates specific bands of current harmonics. While FFT-based methods have shown promise, there are still issues relating to the lack of time information, particularly when considering non-stationary and highly transient nature of DC arc faults.

Time–frequency domain features overcome the disadvantages of solely frequency-based systems by providing the time at which certain harmonics are present. The Short Time Fourier Transform (STFT) and the Discrete Wavelet Transform (DWT) are the most common time–frequency domain methods employed throughout the literature. Chen and Xiong [21], utilise STFT to detect the varying characteristic frequency bands produced by arc noises while Yunmei et al. [22] and Yao et al. [23] evaluate time–frequency signatures of series DC arc fault current extracted using the DWT. However, further opportunities remain to fully explore and utilise the potential of the extracted wavelet coefficients to accurately determine the presence of an arc fault.

Telford et al. [24] use DWT-extracted features as inputs to an advanced machine learning system for the purpose of AFD. However, the study utilises raw DWT coefficients directly to train Hidden Markov Models (HMMs). In general, there is recognition in the literature for the need to employ machine learning (ML) and advanced methods for diagnosis of difficult to detect series arc fault conditions.

Advanced detection systems [25, 26], combining ANN [20], Support Vector Machines [27], and HMM [28], with frequency and time–frequency extracted features, have previously been proposed for series arc fault detection. Detection systems utilising these techniques have the potential to improve upon basic threshold-based systems. However, one drawback is their inherent requirement for access to large volumes of training data. Nonetheless, the volume of data captured within future MEA/MEE systems (test and operational platforms) is expected to be significant [29], improving the prospect for ML-based detection systems to be applied. In Ref. [46], the authors evaluated various ML algorithms that rely on time–domain current as feature extraction for the purpose of AFD and their detection accuracies were compared.

The increased criticality of electrical subsystems within MEA and MEE emphasises the need to overcome these significant AFD challenges and ensure their reliable integration within the aerospace domain. In particular, the presence of dynamic load conditions would be unique to aircraft systems. These issues have previously been discussed in Ref. [2]. Overall, despite extensive propositions of AFD methods within the literature, challenges remain with regards to the following:

- Detection of intermittent arc faults.
- Maintaining performance while accommodating dynamic load conditions.
- Minimisation of false tripping on-board the EPS.
- Optimising the trade-off between diagnostic accuracy and detection time.
- Potential fault masking because of the higher frequency output from power converters and on-board entertainment systems.
- Facilitating a real-time detection methodology.

WaSp utilises time–frequency domain extracted features in combination with Parseval's theorem to obtain the wavelet energy spectra. Highly discriminant features are then chosen, supported by non-parametric kernel density estimates, to be used as inputs to a feed-forward neural network. In this manner, the authors deliver a method that address these remaining key AFD challenges.

3 | WaSp DETECTION METHODOLOGY OVERVIEW

The proposed detection system, WaSp is briefly summarised in Figure 1 and relies on current data that could be sampled at different points on-board an aircraft EPS. The sampled current data then undergoes a 9-level discrete wavelet transform decomposition to produce approximate and detail coefficients. The combination of the wavelet coefficients and Parseval's energy theorem forms the subject for feature extraction. The process is performed over consecutive overlapping windows and utilised as inputs towards a trained feed-forward neural network (NN) for fault diagnosis. Each window has a dimension of 20 ms with a 18 ms overlap and a convergence length of 2 ms. The output from the NN flags the individual window containing fault presence.

The development of the proposed system requires the training of a feed-forward ANN [7]. Training is undertaken in a supervised manner [30], where labelled training cases are provided to the ANN learning algorithms. For the purposes of this paper, an ANN was trained using 5645 separate 20 ms simulated data windows of steady state nominal, arc fault and transient load change conditions. In general, the number of training cases may vary. However, studies into the trade-offs between training data volumes and method performance are out with the scope of this paper.

Prior to ANN training, the sampled current data is transformed to the time–frequency domain using a 9-level discrete wavelet transform. Furthermore, energy is extracted from the wavelet coefficients using Parseval's energy theorem [31]. Analysis of energy levels showed that DWT approximate levels 1–2 and detail levels 2–9 are suitable for discriminating arc fault behaviour.

The following sub-sections describe these aspects in more detail. Section 3.1 discusses arc fault data generation and Section 3.2 outlines feature extraction, analysis and selection. Section 3.3 outlines ANN training, and the applied algorithm for assessing ANN outputs throughout real-time operation is elaborated in Section 3.4.

3.1 | Training data generation

In order to generate suitable training data, arc fault conditions were emulated using a previously validated, empirically derived mathematical model [32]. The model specifically characterises series arc faults in DC systems, including simulation of the electromagnetic transient and stochastic behaviour through arc formation. Each individual simulation run of the model creates varied arcing conditions based upon a stochastic intermittency

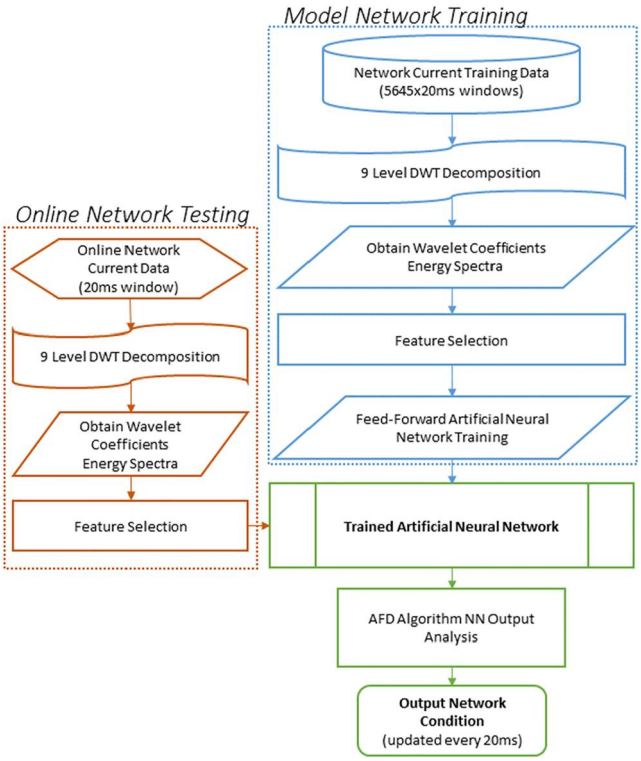

FIGURE 1 Summary of the WaSp arc fault detection (AFD) method

profile, quenching attempts and energy consumption under loading parameters. The fault conditions were simulated on a load feeder using randomised instances of arcing. The speed of electrode separation was varied between 5 mm/s and 25 mm/s and the distance of electrode gap length was randomised between 1 and 15 mm [32]. The system current was sampled at 20 kHz, and a 5 kHz additive Gaussian noise was included in the current profile, representative of on-board interference from on-board power electronics. The authors acknowledge that interference from on-board switching devices will also occur at frequencies higher than 5 kHz. However, it was observed that the 5 kHz sub-band is where most prominent arc features are found. Hence, interference resulting from 5 kHz switching was modelled as a worst-case scenario, where higher frequency switching noise is considered to be less disruptive. The full range of system conditions for the training simulation runs are summarised in Table 1.

For the fault diagnosis system to discriminate accurately between the different system operating conditions, feature extraction and selection is performed on the synthesised network steady-state current data. Selected features are then used as inputs to train the neural network.

3.2 | Feature extraction and selection

Section 2 previously discussed the benefits of transforming raw current data into the time–frequency domain to improve arc fault discrimination. Furthermore, ML-based systems are typically trained using extracted features that best discriminate between different system conditions. This process of feature selection increases accuracy and eliminates data redundancy. The following sub-sections discuss extraction of DWT features from raw current data and outlines the process of selecting optimal features.

3.2.1 | DWT extracted features

The discrete wavelet transform (DWT) extracts frequency components present in a discretely sampled signal through a successive filtering and down-sampling process. Applying the DWT to load current signals, as proposed in this paper, produces approximate and detail coefficients that characterise the variation in time–frequency response of the signal and have the potential to be useful for the purposes of arc fault diagnosis. Furthermore, the analysis of multiple frequency bands is expected to minimise the rate of false positives occurring, for example, as a result of the interference from power electronic switching harmonics. Table 2 outlines the frequency sub-bands of the DWT approximate and detail coefficients for a 20 kHz sampled signal to five decomposition levels. The type of mother wavelet [33] and decomposition level chosen for the signal decomposition affects the obtained sets of approximate and detail coefficients.

For the proposed detection system, the authors undertook a qualitative process to assess the similarity of the decomposed signal with the time domain signal. The raw current signals modelled during arc fault conditions were observed to possess highly transient characteristics and, accordingly, a Daubechies mother wavelet [34] was chosen for extraction purposes. In terms of the decomposition level, it is necessary to select the appropriate level that encompasses a suitable trade-off between the number of distinctive features and computational complexity. For the case presented here, a level 9 decomposition was selected.

Statistical features of the detail and approximate coefficients, such as mean and standard deviation are often used as inputs to advanced fault detection systems. However, these methods are not robust with signals such as current profiles in power distribution systems which contain noise [35]. Hence, the proposed system utilises wavelet energies, obtained using Parseval's theorem [36], for true discrimination between nominal and arc fault conditions.

Equation (1) outlines Parseval's theorem, where $X(f) = \mathscr{F}\{x(t)\}$ is the unitary, normalised continuous Fourier transform of $x(t)$, and f represents the frequency component of x.

$$\int_{-\infty}^{\infty} |x(t)|^2 dt = \int_{-\infty}^{\infty} |X(f)|^2 df \tag{1}$$

Essentially, Parseval's theorem describes the relationship between the energy of the signal and the energy possessed by each detail and approximation level. Therefore, the energy of the time–domain signal, E_{signal}, can be expressed with the

TABLE 1 Arc fault simulation parameters

Model parameter	Value
Electrode gap length	Varied between 1 and 15 mm
Speed of electrode separation	Varied between 5 and 25 mm/s
Sampling rate	20 kHz
Additional simulated noise from on-board sensors	5 kHz Gaussian
DC line resistance	0.641 Ω/km
DC line inductance	0.34 mH/km
DC line capacitance	0.1 μF/km
DC voltage level	270 Vdc
Load resistance	Varied between 5 and 25 Ω
Load inductance	Varied between 1 and 3 mH
DC feeder length	Varied between 45 and 90 m

wavelet approximation and detail coefficient terms through the following Equation (2) [37].

$$E_{\text{signal}} = \sum_{k=-\infty}^{\infty} |c_0(k)|^2 + \sum_{j=0}^{\infty} \sum_{k=-\infty}^{\infty} |d_j(k)|^2 \tag{2}$$

Equation (2) can be rearranged to form (3):

$$E_{\text{signal}} = E_{co} + \sum_{j=0}^{J-1} E_{dj} \tag{3}$$

Where

$$E_{c_0} = \langle c_o(k), c_o(k) \rangle = \|c_{0_2}^2\|$$

$$E_{d_j} = \langle d_j(k), d_j(k) \rangle = \|d_{j_2}^2\| \ .$$

Here, j represents the total number of resolution levels, $c_j(k)$ is the set of scaling function coefficients and $d_j(k)$ is the set of wavelet function coefficients. The signal energy is representative of the energy content at each scale and a higher energy is correlative to more information being present in the decomposition terms. Therefore, the square of the wavelet coefficients of the different levels can aid in the process of feature selection.

3.2.2 | Feature selection

The application of Parseval's theorem to the detail and approximate coefficients highlights the energy disparity between the nominal and fault conditions. Each approximate and detail decomposition energy level is a potential feature that could discriminate between fault and nominal conditions. Non-parametric kernel density estimates (KDE) [38] of energy content at each DWT level were calculated to analyse the distribution of energy across individual 20 ms training windows. KDE analysis of fault and nominal coefficients at each decomposition level determined discriminative features.

TABLE 2 Frequency bands corresponding to approximate and detail coefficients

	Frequency bandwidth	Bandwidth
Time domain signal		
Load current signal	$0 - \frac{f_s}{2}$	0–10 kHz
Time-frequency WT decomposition		
Approximate 1	$0 - \frac{f_s}{4}$	0–5 kHz
Approximate 2	$0 - \frac{f_s}{8}$	0–2.5 kHz
Approximate 3	$0 - \frac{f_s}{16}$	0–1.25 kHz
Approximate 4	$0 - \frac{f_s}{32}$	0–625 Hz
Approximate 5	$0 - \frac{f_s}{64}$	0–312.5 Hz
Detail 1	$\frac{f_s}{4} - \frac{f_s}{2}$	5–10 kHz
Detail 2	$\frac{f_s}{8} - \frac{f_s}{4}$	2.5–5 kHz
Detail 3	$\frac{f_s}{16} - \frac{f_s}{8}$	1.25–2.5 kHz
Detail 4	$\frac{f_s}{32} - \frac{f_s}{16}$	625 Hz–1.25 kHz
Detail 5	$\frac{f_s}{64} - \frac{f_s}{32}$	312.5–625 Hz

The detail coefficients are representative of these high frequency harmonics present in the observed signal. The extracted energy spectra of the training windows of nominal and arc fault data across 9 detail levels of decomposition is shown in Figure 2. Observation of the detail coefficient energy spectra highlighted a notable difference between fault and nominal conditions, particularly at higher decomposition levels. Generally, there is significantly increased energy content present during fault conditions compared to nominal conditions across the decomposition levels 2–9. Inferring from the frequency sub-bands described in Table 2, this confirms that arc conditions result in significant energy at lower frequency sub bands—this supports previous findings described in literature [39, 40].

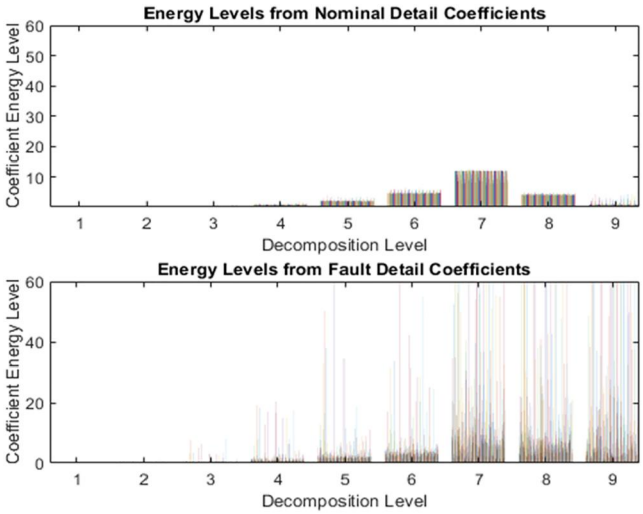

FIGURE 2 Variance in the energy spectra across all detail levels of decomposition for both fault and nominal conditions

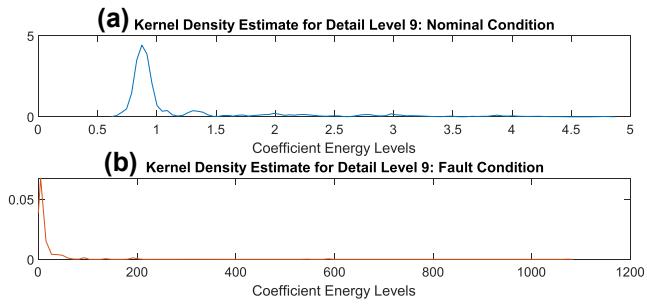

FIGURE 3 Kernel density estimates (KDE) at detail level 9 for (a) nominal condition and (b) for an arc fault condition. Scales readjusted for readability

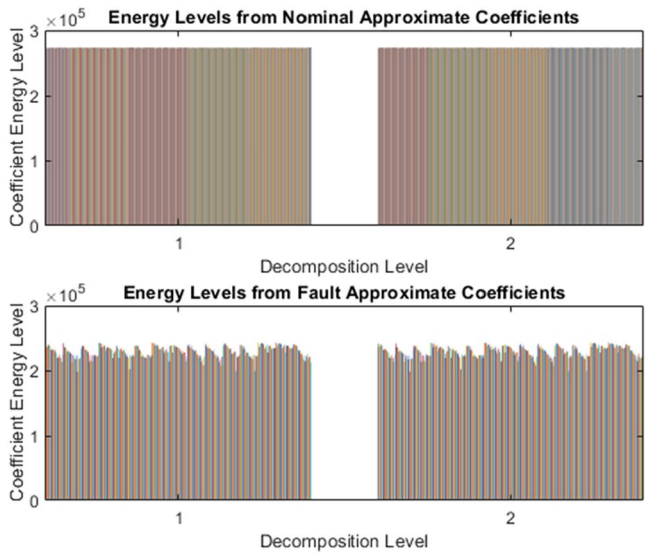

FIGURE 4 Variance in the energy spectra across two approximate levels of decomposition for both fault and nominal conditions

Analysis also highlighted that, as the frequency sub bands narrow (i.e., at higher decomposition levels), there is a higher discrepancy in energy content between fault and nominal conditions.

The non-parametric kernel densities of the detail energy coefficients were analysed. A sample of KDE for individual 20 ms nominal and fault training windows for detail level 9 is shown in Figure 3, highlighting that the magnitude of KDE during fault conditions is significantly higher in comparison to nominal conditions. The coefficient energy levels for a 20 ms window of a nominal condition span from 0.6 to 4.8. Whereas during fault conditions, increased peak densities occur between 0 and 80 while extending up to a maximum of 1150, making the detail level 9 a very useful feature for discrimination criteria.

The detail coefficient energy spectra begin to level out at lower frequency sub-bands as shown in Figure 2, with KDE clustered across certain regions. This was heavily apparent with detail level 1 and was hence, excluded as a feature.

The approximate coefficients extract low frequency harmonics of the current signal at different resolutions. The extracted energy spectra are representative of the original current signal without the high frequency components. Data analysis of the approximate energy spectra of fault conditions show reduced energy content in comparison with nominal conditions. The energy difference between the fault and nominal conditions was consistent across the nine different levels (frequency bands). The peak magnitude for nominal conditions was 2.75×10^5 and for fault conditions was 2.45×10^5. It was observed that the energy spectra remained similar across the several observed levels (1–9). Figure 4 shows the variance in energy content for the extracted training windows (each represented by a different colour) of nominal and fault training data across approximate levels 1 and 2 of decomposition.

The examination of the non-parametric kernel density estimates (KDE) for the approximate levels supported the above conjecture. Figure 5a shows that during the nominal conditions, the approximate coefficient energy showed increased density approximately in the 2.75×10^5 range where the fault condition coefficient energy densities are non-existent. Figure 5b demonstrates the KDE for a fault condition with evidence of good discrimination with higher density between 1.8×10^5 and 2.5×10^5. This highly discriminative behaviour makes for a very useful feature. The repetitive trends observed in the approximate levels makes a case for not utilising all the decomposition levels as inputs. In this case, approximate levels 1 and 2 were selected as input features for WaSp.

3.3 | Artificial neural network (ANN) training

ANNs are non-linear statistical models trained in a supervised manner that use labelled input–output training data [41] to associate ANN weights to a particular condition. WaSp utilises a single-layer feed forward neural network with 20 hidden layer neurons. The number of neurons in the hidden layer was

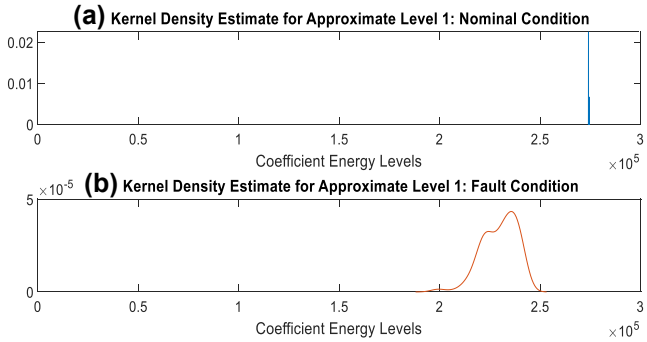

FIGURE 5 Kernel density estimates (KDE) at Approximate level 1 for (a) a nominal condition and (b) for an arc fault condition

chosen based on a continuous trial and error process, and was found to provide maximum stability, a high convergence rate and a minimal training error. The number of neurons was limited throughout this process to reduce computational complexity and also minimise the risk of overfitting [42]. Each of the 10 features described in Section 3.2 were applied as inputs to the ANN. These features included

- Energy of the signal from approximate levels 1 and 2
- Energy of the signal from detail levels 2–9

The training dataset contained 5,645 × 20 ms windows spanning DWT extracted system current data. This included 3395 nominal windows, 990 fault windows and 1260 transient windows. Although, there is variance in sample sizes between the classes, it was deemed there was sufficient data to avoid overfitting issues. The ANN was trained with a scaled conjugate gradient function [43] on the labelled training dataset. The feed-forward neural network utilised for WaSp had two outputs corresponding to fault and nominal system conditions. It was decided that transient conditions would be formed as part of the nominal dataset. Upon the NN outputting a diagnosis, a further analysis is performed by an AFD algorithm for fault inference and is detailed in the following section.

3.4 | Arc fault detection algorithm

To facilitate accurate detection with WaSp, it was necessary to adapt the system towards an MEE/A electrical power system architecture. Hence, a detection scheme was developed in concurrence with the Power Management System (PMS) with the primary intention of minimising the instances of false tripping induced through load switching characteristics. The detection scheme is outlined in Figure 6. The network current data is sampled through a sliding window of 20 ms with intervals of 2 ms and an overlap of 18 ms to be then submitted for the feature extraction and selection process. The utilisation of sliding windows proves advantageous for intermittent arcing events by increasing the likelihood of the detection of changes within the current profile across shorter time periods. The selected features are then fed to the trained neural network for fault diagnosis. During arc fault conditions, the detection system flags the window, n, to be presumptive of a fault. To reduce the likelihood of false positive detections (for example, as a result of converter-produced transients or harmonic content), 10 consecutive flags, $n \geq 10$, are required before a fault trip signal is sent to the appropriate circuit breakers. A further safeguard is also incorporated whereby a real time communication channel from the Power Management System (PMS) is included. This will notify the AFD algorithm of any load changes within the monitored region of the power system, preventing the issue of any fault trip signals during these periods.

4 | PERFORMANCE EVALUATION OF WaSp

The diagnostic accuracy and speed of detection were validated through simulation-based case studies designed to approximate loading conditions on MEE electrical power systems (EPS), although the findings are also extendable to MEA systems. Intermittent series arc faults were injected into the EPS load feeders during static and dynamic load conditions (emulating the operation of fuel pumps, oil pumps, de-icing loads and actuation loads [2]).

The test data from the model simulation was then input to the detection system for fault inference. The outputs were cross-referenced with the known parameters from the test data for verification of the fault diagnosis. The performance of the detection system was evaluated with regards to the following criteria:

- Accurate detection of intermittent arcing events.
- Detection of arcing events with varying degrees of load current magnitude.
- Consistent detection accuracy during step-change and dynamic load change conditions.
- Minimised instances of nominal system conditions resulting in false positive detections.
- Minimal detection times from fault onset.

The detection accuracy was determined to be a function of instances of arcing in the test sample data and the corresponding fault triggers observant from NN diagnosis. Meanwhile, the detection time was the measured time between the fault onset and the earliest fault trigger realised from the NN diagnosis.

A total of 44 simulations were run, the key results of which are summarised in Table 3. All simulation runs spanned over 2 s with intermittent arcing events lasting 120 ms. The case studies evaluated four different scenarios: intermittent series arc fault with no load change, intermittent series arc fault with static load change, intermittent series arc fault with ramped load change, and intermittent series arc fault with oscillatory load behaviour. A brief performance comparison of WaSp with existing methods currently in literature is also provided in Section 5.

4.1 | Case study A: intermittent series DC arc fault with No load change

Case study A evaluates intermittent arc fault events in the sampled current profile occurring under steady state loading conditions. The modelled 270Vdc MEE distribution system consists of both resistive and reactive loads. The series intermittent arc faults were modelled on the load feeders. 10 simulations were run with varying levels of resistance and inductance. The operational voltage was kept constant at 270 Vdc, the equivalent load resistance was varied between 5 and 50 Ω in 5 Ω increments, and load inductance randomised between 1.46 and 2.95 mH. An example simulation run is shown in Figure 7, where the Neural Network analysis shows fault inference directly correspondent to the severity of the intermittent arc. Under these conditions, the proposed system showed a detection rate of 100% with no false positives and averaged detection time of 1.89 ms. The level of impact on the arc fault is very sensitive to the circuit parameters and location of the capacitive filters. In this manner, load capacitors of a few mF or less, or those embedded within LC filters typically have a negligible effect on the arc, whilst larger capacitors lead to more rapid arc extinction (the authors in Ref. [45] also highlight these issues). Unfortunately, the arc model utilised by the authors does not characterise arc extinction events and as such, generates erroneous results under conditions where larger capacitors are used. In either case, the detection of the arc event at the first instance is still critical, and the evaluation of the performance of WaSp against this metric is hence undertaken in the paper.

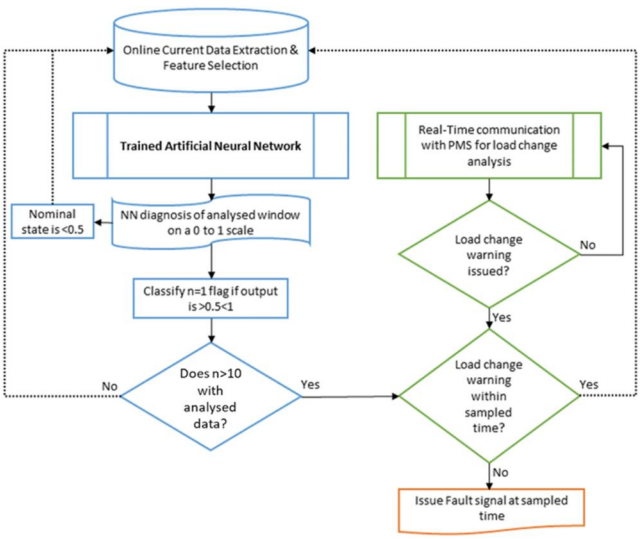

FIGURE 6 Overview of the arc fault detection (AFD) algorithm

4.2 | Case study B: intermittent series DC arc fault with static load change

Case study B, evaluated the impact of stepped load changes (both with load increase and decrease considered) in the sampled current profile on the detection accuracy of the AFD algorithm, resulting in an average accuracy of 90%. The scenarios considering the load switch-on resulted in an average accuracy of 80% across 5 simulations. The scenarios considering load switch-off resulted in an accuracy of 100%, detecting all instances of arcing across 5 simulations. For these, the detection time remained consistent at approximately 1.91 ms. The major transients during step-up load changes could result in potential false positives from the NN output. This case can be seen in Figure 8, where all instances of intermittent arcing are detected and a single false positive detection also occurs during a load switch-on transient. However, with the utilisation of an additional signal input from the power management system, as discussed earlier, it should be possible to ensure that load change conditions do not trigger erroneous fault warnings.

TABLE 3 Case study performance evaluation summary

Test parameter	Total simulations	Operational current (A) range	Variation in test parameter	Average accuracy (%)	Average speed of detection (ms)
Intermittent fault	10	11–97.5 A	N/A	100	1.89
Load switch ON	5	21–51 A	N/A	80	1.91
Load switch OFF	5	21–51 A	N/A	100	1.93
Ramped positive load change	7	6.2–37 A	5–35	100	1.82
Ramped negative load change	7	6.2–37 A	−5 to −25	100	1.91
Oscillatory load current with positive gradient	5	1.2–46.5 A	5–20	100	2.02
Oscillatory load current with negative gradient	5	1.2–46.5 A	−5 to −20	100	1.56
Total	44			97.5	1.86

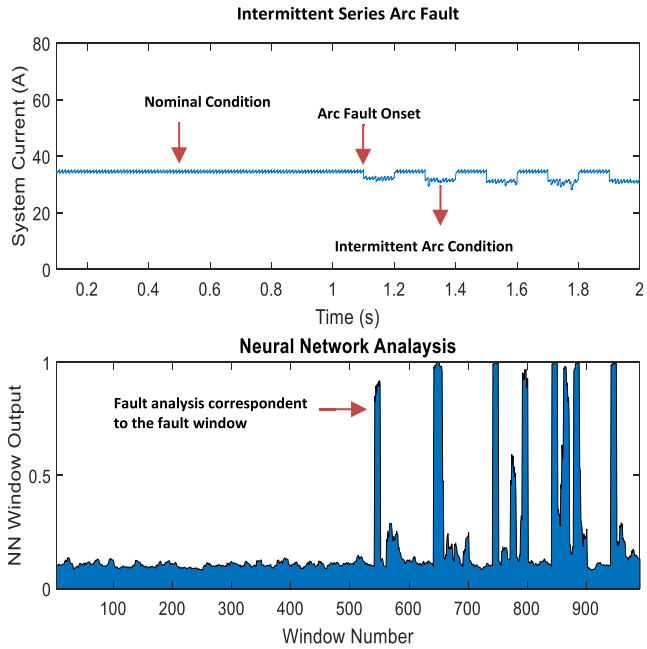

FIGURE 7 Series direct current (DC) Intermittent Arc Fault and the corresponding neural network (NN) Output

4.3 | Case study C: intermittent series arc fault with ramped load change

In case study C, the investigation of the effect of dynamic load changes (i.e., continuously varying load current) on the detection of series intermittent arcs was investigated. This dynamic loading was emulated through the consideration of time snapshots where the load current is ramped up or down at a fixed gradient. The load current ramp gradient was varied from −25 A/s to 25 A/s in increments of 5 A/s. The arc generation model was deemed unstable beyond these limits. The AFD algorithm attained an accuracy of 100% across 10 simulations with an average detection time of 1.87 ms and no instances of false positives. Figure 9 highlights the detection capabilities of the AFD system when inferring intermittent arc faults present in ramped load current profiles.

4.4 | Case study D: intermittent series arc fault with oscillatory load conditions

Finally, case study D investigated the impact of a low frequency sine wave-type current profile (representative of oscillatory load behaviour) on the detection of series intermittent arcing events. The load current amplitude was varied from −20 A/s to 20 A/s at a frequency of 50 rad/sec. The arc generation model was deemed unstable beyond these limits. The operational voltage was 270 Vdc. The results showed 100% accuracy with no instances of false positives. The detection time was shown to be 1.79 ms on average. Figure 10 below, shows a sample of the load current test dataset with the corresponding analysis from the NN.

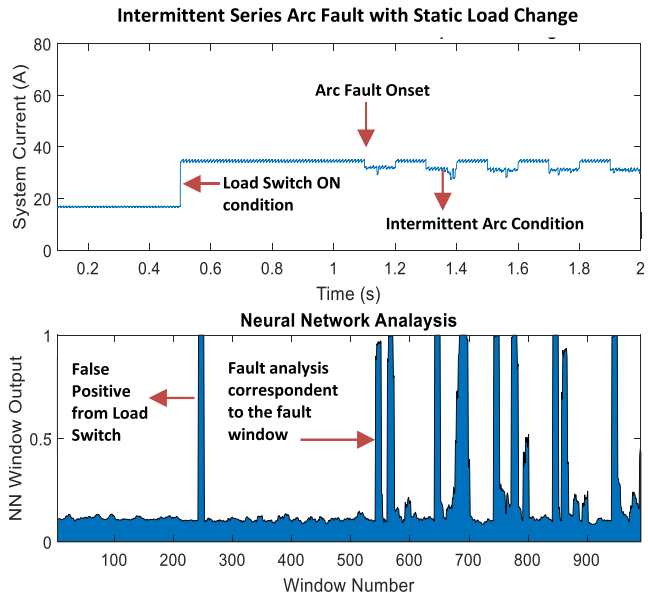

FIGURE 8 Series direct current (DC) Intermittent Arc Fault with Load Switch On and the corresponding neural network (NN) Output

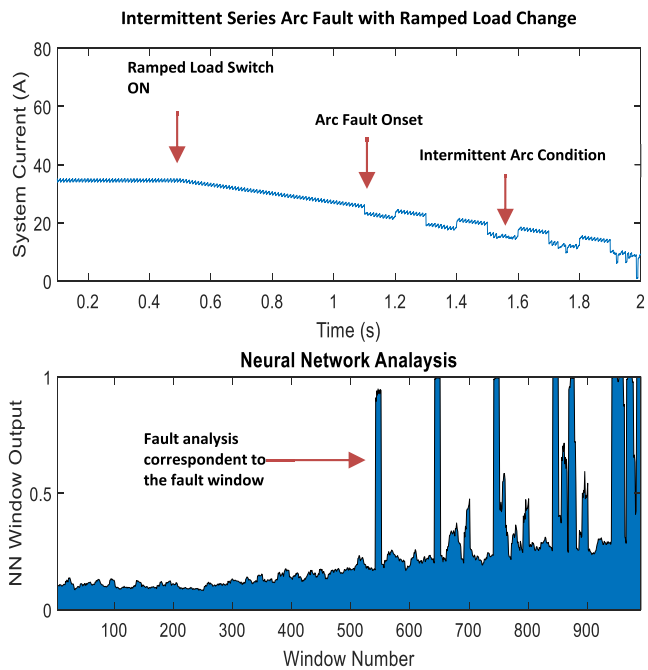

FIGURE 9 Series direct current (DC) Intermittent Arc Fault with Ramp Function Load Current Profile and the corresponding neural network (NN) Output

4.5 | Performance evaluation

Determining the detection and clearance time of series arcs in aircraft applications required to prevent the propagation of arc damage and to hence benchmark the performance of WaSp against is challenging. With a shortage of suitable reference standards specific to aerospace applications, other points of reference must be utilised. The commonly cited IEEE 1584 [47]

provides a model for determining arc energy and arc flash boundary as a function of a number of parameters, including arc duration. While the valid range of the model's electrical parameters does not align well with aerospace applications, it does still provide useful examples of the impact of arc duration, where a particular case study shows that a 100 ms arcing event leads to an arc boundary of 4.4 inches, while a 10 ms arcing event of otherwise similar nature results in a 1.5 inch boundary. However, authors in Ref. [48] raised concerns that the model may be overly cautious, a point reinforced by the study in Ref. [49] where an experiment run on 270VDC aircraft wiring with an arc duration of less than 200 ms characterised the arc boundary as being only 0.5 inches [49].

In the absence of consistent absolute restrictions on clearance times, there is instead an onus to consistently detect and clear arc faults as quickly as possible. In this manner, the determined arc boundary is used to set the clearance distances between wiring and other components required in order to prevent the propagation of fault damage. Creating larger separation distances is challenging in aircraft systems in general, and this may be further exacerbated in physically compact applications such as MEE systems. In terms of detection time, WaSp has shown an average detection time of 1.86 ms which is a modest improvement compared with state-of-the-art AI-based detection methods [23, 28] and deterministic based detections methods [45].

It is also worth comparing this detection time with typical circuit breaker operating times for further context. Compared to typical mechanical circuit breaker operating times of 10–200 ms, the detection time of WaSp is largely insignificant. For quicker operating SSPCs (with clearance times of much less than 1 ms), the detection time of WaSp is still at least comparable.

Finally, from the perspective of fault effects propagating electrically (i.e. as a result of a sustained downstream undervoltage), the WaSp detection time is consistent with trip times for typical short circuit protection devices (thermal/i2t etc.) and would comfortably comply with the maximum acceptable abnormal transients as stipulated in Mil 704F [50].

5 | COMPARISON WITH EXISTING AFD METHODS

WaSp addresses several drawbacks observed within existing AFD methodologies. For example, in Ref. [20], the authors utilise FFT extracted features with a backpropagation ANN for AFD purposes. However, it showed very limited diagnostic accuracy with only 40% of the 5 fault case scenarios correctly diagnosed. The testing parameters also did not incorporate transient load changes. This highlights the drawbacks present with frequency domain-based feature extraction when observing transient and non-stationary signals such as arc faults. In comparison, WaSp showed a higher degree of accuracy of 97.5% across 44 test case scenarios while accounting for several transient load change parameters.

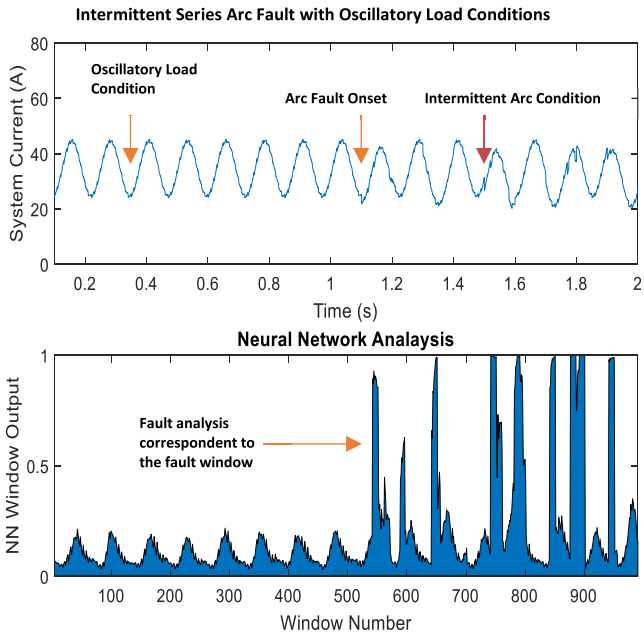

FIGURE 10 Series direct current (DC) Intermittent Arc Fault with Oscillatory Load Current and the corresponding neural network (NN) Output

An AFD method that combines time and time-frequency domain extracted features [44] showed high accuracy albeit at lower operational voltages and current levels. It demonstrated an accuracy of 40% at 240 Vdc and 60% at 300 Vdc. The case study also did not take intermittent arc faults into consideration and did not address performance under dynamic loading conditions. This paper evaluated the performance of WaSp under reactive and dynamic load conditions typical of MEE system operation, at 270 Vdc.

In Ref. [23], the authors present a methodology that utilises wavelet packet analysis for LVDC AFD. Although the system showcased high accuracy, the generalisation of the system is less robust as the load profiles were not varied throughout the case studies. The IntelArc method [28] exhibited highly accurate fault diagnosis under conditions applicable to an MEA EPS. It performed well in the presented case studies, including transient loading conditions in both simulated and hardware testbeds. However, it is seen to have a higher detection time than WaSp under similar testing conditions and its performance under dynamic loading conditions was not evaluated. The deterministic detection method for series arcing, using load side voltage drop for protection of low voltage DC systems is presented in Ref. [45]. This method provides fast detection times similar to those achieved by the WaSp method. However, the authors of Ref. [45] do note that the detection effectiveness of the method is sensitive to the levels of local circuit inductance and capacitance, whereas WaSp has shown a good degree of immunity to circuit parameters. Ultimately, the authors believe however, that this voltage drop method and WaSp display a good degree of complementarity, and their combined utilisation could perhaps offer a reliable implementation route for future platforms.

6 | FURTHER WORK

As part of the plans for further work, the authors intend to extend the training dataset and test the WaSp methodology on hardware generated data. However, facilitating data generation at the prescribed voltage levels for the MEA system may not be feasible due to safety and resource accessibility reasons. Therefore, scaling down the operational voltage while maintaining equivalent current levels is potentially the most appropriate measure. The application WaSp on a microcontroller or FPGA platform in pursuit of a live detection system is another area of interest. Online test data would be extracted, processed, and analysed via the microcontroller/FPGA in lieu to communicate with solid state power controllers (SSPCs) to isolate the fault. This would provide further information on the overall speed of fault detection and isolation.

Certification of ML-based methods on-board MEE/MEA systems may prove to be difficult due to the inherent probabilistic component involved with fault diagnosis. Further development of the detection scheme that combines a deterministic element with the proposed system may be necessary to meet certification standards. The prioritisation of the deterministic and probabilistic system in a hierarchical system may prove to be challenging. However, as the MEE/MEA concepts develop further, aircraft system integrators are likely to evolve the current certification standards to accommodate AI-based on-board systems. One complementary approach could be the implementation of AI detection systems as a health monitoring and diagnostics function, where the fault response action is undertaken by maintenance personnel. This indirect causality between detection and response may be more acceptable from a certification perspective. Extended use of probabilistic methods in this capacity could also help to increase confidence in their subsequent direct use. In addition, some low-energy highly intermittent series arcing events may develop over a period of several flights, in essence, manifesting more as a health management issue and necessitating the use of highly sensitive, trend-based health monitoring approaches.

7 | CONCLUSION

An AFD method (WaSp) has been proposed for the detection of intermittent series arc faults observant on-board DC MEE/MEA systems. The utilisation of an ML-based approach was motivated by the demand to handle large volumes of data in future aircraft EPS and the ability to generalise detection across a wide range of network conditions. Case studies pertaining to MEA EPS system conditions were utilised to assess the performance of the proposed methodology. The case studies investigated diagnosis accuracy and speed of detection during load profiles that are representative of the fuel pumps, actuation loads and de-icing loads of an MEE EPS. Finally, thoughts on further development of the WaSp with consideration of current MEA certification standards were provided.

Although series intermittent arc faults are widely regarded as a dangerous phenomenon in aircraft applications, further work is still required to realise reliable protection coverage against these fault types. Furthermore, greater consideration of the application of the AFD technique to a specific operating domain, architecture and conditions is required. As an alternative to developing novel techniques that address certain challenges that persists within the AFD system, it might be advantageous exploring sub-level systems within the operational domain architecture. An example is the utilisation of the PMS in a hybrid manner to mitigate against false positive detections during load switching conditions as shown in this paper. It is the authors' opinion that there may be substantial whole-system benefits if arc fault detection systems are supported or even integrated with other EPS subsystems rather than considered as a standalone entity.

ACKNOWLEDGEMENT

This work was carried out as part of the Rolls-Royce University Technology Centre programme.

CONFLICT OF INTEREST

The authors declare no conflict of interests.

DATA AVAILABILITY STATEMENT

Data used to support the findings of this study are included within the article.

PERMISSION TO REPRODUCE MATERIALS FROM OTHER SOURCES

None.

ORCID

J. Thomas https://orcid.org/0000-0001-9677-1528

REFERENCES

1. Yitao Liu, S.L., Deng, J., Liu, C.: Energy optimization analysis of the more electric aircraft Energy optimization analysis of the more electric aircraft. IOP Conf. Ser. Earth Environ. Sci. (2017)
2. Hirst, M., et al.: Demonstrating the more electric engine: a step towards the power optimised aircraft. IET Electr. Power Appl. 5(1), 3 (2011). https://doi.org/10.1049/iet-epa.2009.0285
3. Hammerstrom, D.J.: AC versus DC distribution systems-did we get it right? In: IEEE Power Eng. Soc. Gen. Meet. PES, pp. 1–5 (2007)
4. Yaramasu, A., et al.: Aircraft electric system intermittent arc fault detection and location. IEEE Trans. Aero. Electron. Syst. 51(1), 40–51 (2015). https://doi.org/10.1109/taes.2014.120556
5. Traskos, M.: F-22 Crash and Aircraft Electrical Arcing. Accessed on 07 June 2021
6. Lu, S., Phung, B.T., Zhang, D.: A comprehensive review on DC arc faults and their diagnosis methods in photovoltaic systems. Renew. Sustain. Energy Rev. 89, 88–98 (2017). https://doi.org/10.1016/j.rser.2018.03.010
7. Sazli, M.H.: A brief review of feed-forward neural networks. Commun. Fac. Sci. Univ. Ankara, no. May, 11–17 (2006), https://doi.org/10.1501/0003168
8. Stokes, A.D., Oppenlander, W.T.: Electric arcs in open air. J. Phys. D Appl. Phys. (1991)
9. Müller, P., et al.: Current characteristics of serial and parallel low current arc faults in distribution networks possible arc faults in switchgear. In: 21 St International Conference on Electricity Distribution Frankfurt, 6–9 (2011)
10. Kuhn, P.K., Furse, C., Smith, P.: Locating hidden hazards in electrical wiring. Aged Electr. Syst. Res. Appl. Symp., 1–8 (2006)

11. Tomimbang Wendell, E.: Arc Fault Circuit Interrupter, Systems, Apparatus and Methods of Detecting and Interrupting Electrical Faults (2010)
12. Brusso, B.C.: History of aircraft wiring arc-fault protection. IEEE IN Appl. Mag. 23(3), 6–11 (2017). https://doi.org/10.1109/mias.2017.2659022
13. Frederick, K., Blades: Series arc fault diagnostic for aircraft wiring, vol. 2(12) (2001)
14. Ohta Yoshito Ise-shi Mie and Isoda Hirotaka Ise-shi Mie. Arc Detecting device and aircraft equipped therewith, vol. 1(19), pp. 1–27 (2009)
15. Andrea, J., Zirn, O., Bournat, M.: Principle of arc fault detection for solid state power controller. (2012)
16. Chen, S., et al.: Detection of series DC arc fault using rogowski coil. Annu. Rep. - Conf. Electr. Insul. Dielectr. Phenomena, CEIDP 2018, 401–404 (2017)
17. Chen, M., et al.: Detection method of low voltage series DC arc based on the pattern matching algorithm. Int. Conf. Electr. Mach. Syst. ICEMS (2017)
18. Kojori, H., Li, C., and Dawson, F., Method and Apparatus for Generalized Arc Fault Detection, no. US20060203401 A1. Sep (2006)
19. Momoh, J., Button, R.: Design and analysis of aerospace DC arcing faults using fast Fourier transformation and artificial neural network. Power Eng. Soc. Gen., 788–793 (2003)
20. Cai, X., et al.: AC arc fault detection based on mahalanobis distance. In: 15th Int. Power Electron. Motion Control Conf. Expo, pp. 1–6. EPE-PEMC 2012 ECCE Eur. (2012)
21. Chen, S., Li, X., Xiong, J.: series arc fault identification for photovoltaic system based on time-domain and time-frequency-domain analysis. IEEE J. Photovoltaics 7(4), 1105–1114 (2017). https://doi.org/10.1109/jphotov.2017.2694421
22. Yunmei, G., et al.: Wavelet packet analysis applied in detection of low-voltage DC arc fault. In: 2009 4th IEEE Conf. IN Electron. Appl. ICIEA, vol. 2(1), pp. 4013–4016 (2009)
23. Yao, X., Herrera, L., Wang, J.: A series DC arc fault detection method and hardware implementation. In: 28thAnnual IEEE Applied Power Electronics Conference and Exposition, pp. 2444–2449. (APEC) (2013)
24. Telford, R.: Novel methods for improving fault protection & health management within advanced aircraft electrical power systems. PhD diss. University of Strathclyde (2017)
25. Grichting, B., Goette, J., Jacomet, M.: Cascaded fuzzy logic based arc fault detection in photovoltaic applications In: 5th Int. Conf. Clean Electr. Power Renew. Energy Resour. Impact, vol. 2015, pp. 178–183. ICCEP (2015)
26. Wang, Z., Balog, R.S.: Arc Fault and Flash Detection in Photovoltaic Systems Using Wavelet Transform and Support Vector Machines. IEEE 43rd Photovolt. Spec. Conf., pp. 3275–3280. (2016)
27. Yang, K., et al.: A novel arc fault detector for early detection of electrical fires. Sensors 16(4), 500 (2016). https://doi.org/10.3390/s16040500
28. Telford, R.D., et al.: Diagnosis of series DC arc faults—a machine learning approach. IEEE Trans. Ind. Inf. 13(4), 1598–1609 (2017). https://doi.org/10.1109/tii.2016.2633335
29. Maggiore, J.B.: Remote management of real-time airplane Data. Boeing AERO Quarterly 27, 22–25 (2007)
30. Sathya, R., Abraham, A.: Comparison of supervised and unsupervised learning algorithms for pattern classification. Int. J. Adv. Res. Artif. Intell. 2(2), 34–38 (2013). https://doi.org/10.14569/ijarai.2013.020206
31. Kelkar, S.S., Grigsby, L.L., Langsner, J.: An extension of Parseval's theorem and its use in calculating transient energy in the frequency domain. IEEE Trans. Ind. Electron. 1, 42–45 (1983). 10.1109/TIE.1983.356702
32. Uriarte, F.M., et al.: A DC arc model for series faults in low voltage microgrids. IEEE Trans. Smart Grid 3(4), 2063–2070 (2012)
33. Ngui, W.K., et al.: Wavelet analysis: mother wavelet selection methods. Appl. Mech. Mater. 393, 953–958 (2014). https://doi.org/10.4028/www.scientific.net/amm
34. Vonesch, C., et al.: Generalized Daubechies wavelet families. IEEE Trans. Signal Process. 55(9), 4415–4429 (2007). https://doi.org/10.1109/tsp.2007.896255
35. Demir, Y.: Wavelet-based feature extraction and selection for classification of power system disturbances using support vector machines, vol. 80, pp. 743–752 (2010)
36. Liao, C., Yang, H.: Recognizing noise-influenced power quality events with integrated feature extraction and neuro-fuzzy network. IEEE Trans. Power Deliv. 24(4), 2132–2141 (2009). https://doi.org/10.1109/tpwrd.2009.2016789
37. Gaouda, A.M., et al.: Monitoring HVDC systems using wavelet multi-resolution analysis 16(4), 662–670 (2001)
38. Beardahy, M.J.B., C, C.: 1 Introduction 2 the Mathematics of KDEs. Statistics (Ber) (1988)
39. Parker, M.T., et al.: Electric arc monitoring systems, no. US6772077 B1, (2004)
40. Thomas, J., et al.: DC arc fault detection methods in MEA distribution systems. In Aerospace Systems and Technology Conference, vol. November, (2018)
41. Jain, A.K., Mao, J., Mohiuddin, K.M.: Artificial neural networks: a tutorial. Computer 29(3), 31–44 (1996). https://doi.org/10.1109/2.485891
42. Mathworks: Machine Learning Challenges: Choosing the Best Model and Avoiding Overfitting, pp. 1–8 (2016)
43. Meiller, M.F.: A scaled conjugate gradient Algorithm for Fast Supervised Learning. Neural networks 6, 525–533 (1993)
44. Yao, X., et al.: Characteristic study and time domain-discrete wavelet transform based hybrid detection of series DC arc faults. IEEE Trans. Power Electron. 29(6), 3103–3115 (2014). https://doi.org/10.1109/tpel.2013.2273292
45. Aditya, S., et al.: Detection of series arcs using load side voltage drop for protection of low voltage DC systems. IEEE Trans. Smart Grid 9(6), 6288–6297 (2017). https://doi.org/10.1109/tsg.2017.2707438
46. Hoang-Long, D., et al.: Series DC arc fault detection using machine learning algorithms. IEEE Access 9, (2021)
47. IEEE 584 Arc-Flash Hazard Calculation for Arc Flash Safety IEEE Standards 1584-2002, (2002)
48. Traskos, M.: IEEE 1584-Arc Standard Lectromec (2020). https://www.lectromec.com/ieee-1584-arc-standard. Accessed on 26 May 2022
49. Traskos, M.: 270VDC Arcing in Aircraft Wiring Lectromec (2014). https://www.lectromec.com/270vdc-arcing-in-aircraft-wiring. Accessed on 26 May 2022
50. Department of Defense Interface Standard: MIL-STD-704F: Aircraft Electrical Power Characteristics. Department of Defense Interface Standard (2004)

How to cite this article: Thomas, J., et al.: Intermittent series direct current arc fault detection in direct current more-electric engine power systems based on wavelet energy spectra and artificial neural network. IET Electr. Syst. Transp. 1–12 (2022). https://doi.org/10.1049/els2.12047